Steady state analysis of short-term exchange of leader-laggard relationship in chaotic synchronized semiconductor lasers with low-frequency fluctuations

Kazutaka Kanno[1,2], Takuya Hida[1], Atsushi Uchida[1], and Masatoshi Bunsen[2]

[1]Department of Information and Computer Sciences, Saitama University,
255 Shimo-Okubo, Sakura-ku, Saitama City, Saitama, 338-8570, Japan
[2]Graduate School of Engineering, Fukuoka University, 8-19-1 Nanakuma, Johnan-ku, Fukuoka 814-0180, Japan
Email: kkanno@fukuoka-u.ac.jp, owenaguero7@gmail.com, auchida@mail.saitama-u.ac.jp

Abstract—We investigate synchronized dynamics of mutually-coupled semiconductor lasers with low frequency fluctuations (LFFs). The mutually-coupled semiconductor lasers show the repeated spontaneous switching of leader-laggard relationship. Leader-laggard relationship is the phenomenon that one system in synchronized mutually-coupled dynamical systems oscillates forward and is called "leader," and other system is called "laggard." We observe that the leader-laggard relationship is inverted repeatedly at the propagation delay time interval and explain the phenomenon by using the analysis of steady state solution in the Lang-Kobayashi equations for the dynamics of semiconductor lasers. We found that the optical frequency of one laser attracts that of another laser, and the leader-laggard relationship is exchanged repeatedly .

1. Introduction

Synchronization of chaos has been intensively investigated in coupled nonlinear dynamical systems [1, 2], such as optically coupled semiconductor lasers [3, 4]. Lag synchronization has been reported in mutually-coupled semiconductor lasers with time delayed coupling [5–7]. This phenomenon is known as the leader-laggard relationship, where one of the two coupled lasers oscillates in advance to the other laser by the propagation delay time of the light. The laser oscillating in advance is called "the leader," and the other laser is called "the laggard." The role of leader-laggard relationship is dependent of the optical frequency detuning and the coupling strength. Recently, short-term exchange of the leader-laggard relationship has been reported [8], where the leader-laggard relationship exchanges in time for every propagation delay times. However, the mechanism of the short-term exchange of the leader-laggard relationship has not been well investigated yet.

In this study, we investigate the short-term exchange of the leader-laggard relationship for the dynamics of low-frequency fluctuations (LFFs) in mutually-coupled semiconductor lasers. We calculate steady state solutions of the Lang-Kobayashi equations for mutually-coupled semiconductor lasers to understand the relationship between the short-term exchange and the LFF dynamics [9, 10].

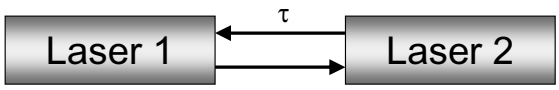

Figure 1: Model for mutually-coupled semiconductor lasers with time delay. τ is the propagation delay time of the light.

2. Numerical model

Figure 1 shows a model for mutually-coupled semiconductor lasers. The optical output from the laser 1 is injected into the laser 2 after the propagation delay time τ of the light. The output of the laser 2 is also injected into the laser 1. This coupled system is considered as an infinite dimensional system due to the existence of the coupling delay time. It is expected to observe synchronization of chaos in numerical simulations. We show a numerical model known as the Lang-Kobayashi equations for semiconductor lasers with time-delayed optical coupling [11].

$$\frac{dE_{1,2}(t)}{dt} = \frac{1+i\alpha}{2}\left[\frac{G_N(N_{1,2}(t)-N_0)}{1+\varepsilon|E_{1,2}(t)|^2} - \frac{1}{\tau_p}\right]E_{1,2}(t) + \kappa E_{2,1}(t-\tau)\exp\left[i\theta_{1,2}(t)\right] \quad (1)$$

$$\frac{dN_{1,2}(t)}{dt} = J - \frac{N_{1,2}(t)}{\tau_s} - \frac{G_N(N_{1,2}(t)-N_0)}{1+\varepsilon|E_{1,2}(t)|^2}|E_{1,2}(t)|^2 \quad (2)$$

$$\theta_{1,2}(t) = (\omega_{2,1}-\omega_{1,2})t - \omega_{2,1}\tau \quad (3)$$

where E and N are the slowly varying complex electric-field amplitude and the carrier density of the semiconductor lasers, respectively. The subscripts 1 and 2 represent the laser 1 and 2, respectively. $\alpha = 3$ is the linewidth enhancement factor, G_N is the gain coefficient, N_0 is the carrier density at transparency, and ϵ is the gain saturation coefficient. τ_p and τ_s are the photon and the carrier lifetimes, respectively. $J = 1.2J_{th}$ is the injection current of the lasers, where J_{th} is the injection current at the lasing threshold. The second term in the right-hand side of Eq. (1) represents the optical injection from the other laser. κ is the coupling strength between the two lasers and τ is the propagation delay time of the light. $\theta_i(t)$ $(i = 1, 2)$ is the optical phase difference between the two lasers. In Eq. (3)

for $\theta_i(t)$, $\Delta\omega$ is the optical angular frequency detuning between the laser 1 and 2, and is defined as $\Delta\omega = \omega_1 - \omega_2$, where ω is the optical angular frequency of the laser. The following parameter values are used in our numerical simulations: $\kappa = 31.06\ \mathrm{ns}^{-1}$, $\tau = 1$ ns, and the optical frequency detuning $\Delta f = \Delta\omega/(2\pi) = 2$ GHz. Other parameter values are set to be the same as in Ref. [12].

3. Steady State Solution

We show steady state solutions of the Lang-Kobayashi equation (1) and (2) for the mutually-coupled semiconductor lasers. We define the steady state solutions of $E_{1,2}(t)$ and $N_{1,2}(t)$ as $E_{s1,s2} = A_{s1,s2}\exp[i(\omega_{s1,s2} - \omega_{1,2})t]$ and $N_{s1,s2}$, respectively. $A_{s1,s2}$ is the steady state solution of the electric-field amplitude of $E_{1,2}$. $\omega_{s1,s2}$ is the steady state solution of the optical angular frequency. The following equations are obtained by inserting these solutions into Eq. (1) and (2) and by dividing the complex variables into the real and imaginary parts.

$$0 = \frac{1}{2}\left[\frac{G_N(N_{s1,s2} - N_0)}{1 + \epsilon|A_{s1,s2}|^2} - \frac{1}{\tau_p}\right] + \kappa\frac{A_{s2,s1}}{A_{s1,s2}}\cos\theta_{s1,s2}(t) \quad (4)$$

$$\omega_{s1,s2} - \omega_{1,2} = \frac{\alpha}{2}\left[\frac{G_N(N_{s1,s2} - N_0)}{1 + \epsilon|A_{s1,s2}|^2} - \frac{1}{\tau_p}\right] - \kappa\frac{A_{s2,s1}}{A_{s1,s2}}\sin\theta_{s1,s2}(t) \quad (5)$$

$$0 = J - \frac{N_{s1,s2}}{\tau_s} - \frac{\alpha}{2}\frac{G_N(N_{s1,s2} - N_0)}{1 + \epsilon|A_{s1,s2}|^2}|A_{s1,s2}|^2 \quad (6)$$

$$\theta_{s1,s2}(t) = (\omega_{s2,s1} - \omega_{s1,s2})t + \omega_{s1,s2}\tau \quad (7)$$

Note that Eq. (7) for $\theta_{s1,s2}(t)$ includes the time t. From the requirement of constant $\theta_{s1,s2}(t)$ for the time t, $\omega_{s1} = \omega_{s2}$ need to be satisfied. This requirement indicates that injection locking is achieved between the two coupled lasers. We obtain the following conditions for the steady state solutions from Eqs. (4)–(7) and $\omega_{s1} = \omega_{s2} = \omega_s$.

$$(\omega_s - \omega_1)(\omega_s - \omega_2) = \frac{\kappa^2(1+\alpha^2)}{2}(1 - \cos[2(\omega_s\tau + \tan^{-1}\alpha)]) \quad (8)$$

$$N_{s1,s2} - N_{th} = \frac{2\kappa^2\tau_s\sqrt{1+\alpha^2}\cos[\omega_s\tau]\sin[\omega_s\tau + \tan^{-1}\alpha]}{(G_N\tau_s + \epsilon)\Delta\omega_{s2,s1}} + \frac{\epsilon N_{th}(j-1)}{G_N\tau_s + \epsilon} \quad (9)$$

Where N_{th} is the carrier density at the lasing threshold ($N_{th} = N_0 + 1/(G_N\tau_p)$).

4. Numerical results

Figure 2 shows the temporal waveform of the mutually-coupled semiconductor lasers. We show the dynamics of the laser intensity $I(t) = E_{re}^2(t) + E_{im}^2(t)$, where E_{re} and E_{im}

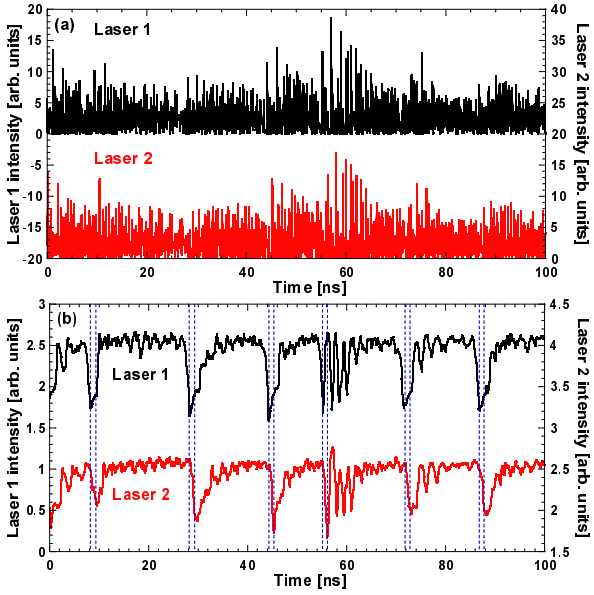

Figure 2: (a) Temporal waveforms of $I(t)$ for the mutually-coupled semiconductor lasers. The black and red curves represent the laser 1 and 2, respectively. (b) Low-pass filtered temporal waveforms of (a). A third-order low-pass filter with the cut-off frequency of 0.5 GHz is used.

are the real and imaginary parts of E, respectively. Figures 2(a) and (b) show the original and low-pass filtered waveforms, respectively. The upper curve (the black curve) represents the laser 1 and the lower one (the red curve) represents the laser 2. We can observe fast oscillations over a few GHz for both the upper and lower curves in Fig. 2(a). Low frequency fluctuations (LFFs) can be clearly observed as sudden intensity dropouts in low-pass filtered waveforms of Fig. 2(b). The leader-laggard relationship can be determined with the order of the dropouts of the two lasers. In Fig. 2(b), the dropouts of the laser 1 always occurs in advance, indicating that the laser 1 is the leader. The leader is determined by the sign of the optical frequency detuning Δf. Positive frequency detuning $\Delta f > 0$ (i.e., $f_1 > f_2$) in Fig. 2 results in the leader of the laser 1.

To investigate short-term exchange of the leader-laggard relationship, we calculate the two short-time cross correlations as follows,

$$C_1(t) = \frac{\left\langle\left[I_1(t-\tau) - \bar{I}_1(t-\tau)\right]\left[I_2(t) - \bar{I}_2(t)\right]\right\rangle}{\sigma_1(t-\tau)\sigma_2(t)} \quad (10)$$

$$C_2(t) = \frac{\left\langle\left[I_1(t) - \bar{I}_1(t)\right]\left[I_2(t-\tau) - \bar{I}_2(t-\tau)\right]\right\rangle}{\sigma_1(t)\sigma_2(t-\tau)} \quad (11)$$

where 1 and 2 represent the laser 1 and 2, respectively. $\bar{I}(t)$ is the mean of the laser intensity for $[t-\tau, t]$. $\sigma(t)$ is the standard deviation of the intensity for $[t-\tau, t]$. $\langle\cdot\rangle$ represents the time averaging for $[t-\tau, t]$. $C_1(t)$ is the cross correlation function between $I_1(t-\tau)$ and $I_2(t)$. On the contrary, $C_2(t)$ is

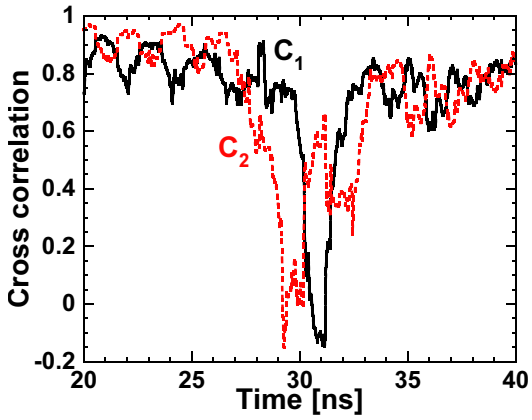

Figure 3: Temporal waveforms of the short-term cross correlations $C_1(t)$ and $C_2(t)$. The black solid and red dashed curves represent $C_1(t)$ and $C_2(t)$, respectively. The temporal waveforms in Fig. 2(a) are calculated from 20 to 40 ns.

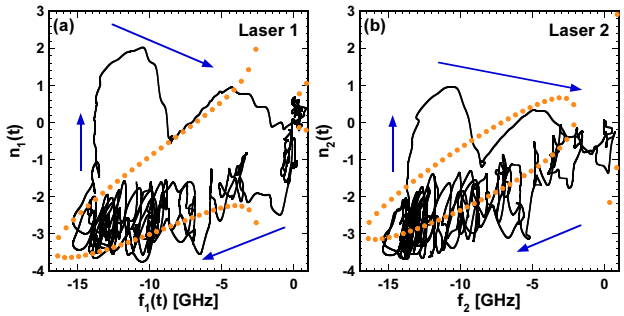

Figure 4: Trajectories of the low-frequency fluctuations of the mutually coupled lasers in the phase space for (a) laser 1 and (b) laser 2. The phase space consists of the optical frequency and the carrier density. The orange circles indicate the steady state solutions. The blue arrows represent the direction of change in the trajectories.

the cross correlation function between $I_1(t)$ and $I_2(t-\tau)$. We can determine the leader by using the sign of $C_1(t) - C_2(t)$. The laser 1 is the leader for $C_1(t) - C_2(t) > 0$, and the laser 2 is the leader for $C_1(t) - C_2(t) < 0$.

Figure 3 shows the temporal waveforms of $C_1(t)$ and $C_2(t)$, calculated from the temporal waveforms in Fig. 2(a) from 20 to 40 ns . $C_2(t)$ decreases at 29 ns and $C_1(t)$ remains high correlation when the sign of $C_1(t)-C_2(t)$ is positive and the laser 1 is leader, as shown in Fig. 2(b). Next, $C_1(t)$ decreases at 31 ns when the sign of $C_1(t) - C_2(t)$ becomes negative at 31 ns and the laser 2 becomes the leader. After that, the sign of the correlations is changed for every propagation delay times τ, and leader-laggard relationship is exchanged alternately. This is an indication of the short-term exchange of leader-laggard relationship.

To understand the short-term exchange, we investigate

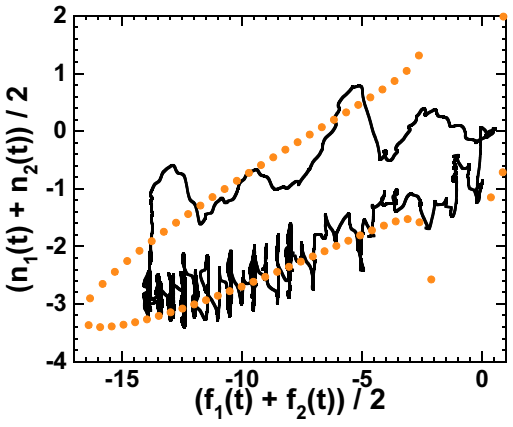

Figure 5: Averaged trajectory of the two coupled lasers in the phase space. The orange circles indicate the averaged steady state solutions.

the relationship between steady state solutions and trajectory of the low-frequency fluctuations of the mutually coupled lasers in the phase space. Figure 4 shows the attractor and the steady state solutions of the mutually coupled lasers in the phase space. Figures 4(a) and (b) represent the laser 1 and 2, respectively. The horizontal axis corresponds to the optical frequency $f_{1,2}(t)$ calculated from the optical phase $\phi_{1,2}(t)$ as follows.

$$f_1(t) = \frac{\phi_1(t) - \phi_1(t-\tau)}{2\pi\tau} \tag{12}$$

$$f_2(t) = \frac{\phi_2(t) - \phi_2(t-\tau)}{2\pi\tau} - \Delta f \tag{13}$$

where $\phi(t) = \tan^{-1}[E_{im}(t)/E_{re}(t)]$. The vertical axis is the normalized carrier density $n_{1,2}(t) = 100(N_{1,2}(t) - N_{th})/N_{th}$. The orange circles in Fig. 4 indicate the steady state solutions of the optical frequency $f_s = \omega_s/(2\pi)$ and the normalized carrier density $n_{s1,s2} = 100(N_{s1,s2} - N_{th})/N_{th}$.

The intensity dropout occurs around $f_{1,2}(t) \approx -14$ GHz, where $n_{1,2}(t)$ suddenly increases. After the increase of $n_{1,2}(t)$, the trajectory moves to the direction of the blue arrow and the optical frequency $f_{1,2}(t)$ increases to zero. The trajectory slowly moves to the negative direction of the optical frequency along the lower steady state solutions after the trajectory arrives at $f_{1,2} \approx 0$. The above-described cycle is repeated. A single semiconductor laser with optical self-feedback shows a similar behavior in the LFF dynamics [9, 10].

Next, we investigate the averaged trajectory and the steady state solutions for the laser 1 and 2, as shown in Fig. 5. The averaged trajectory and complete-synchronization solutions in mutually-coupled semiconductor lasers have been investigated in [6]. However, in our case, the optical frequency detuning Δf needs to be taken into account. The horizontal axis of Fig. 5 represents $(f_1(t) + f_2(t))/2$ and the vertical axis represents $(n_1(t) + n_2(t))/2$. The steady state solutions of the carrier density are also averaged as

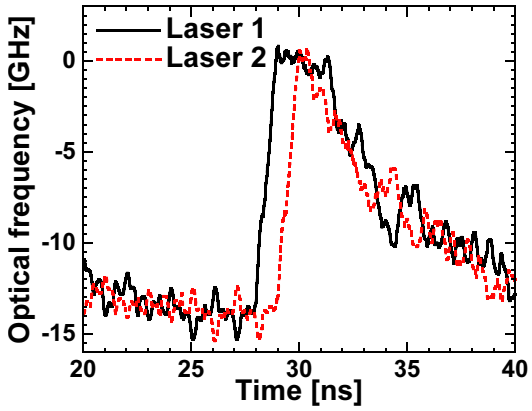

Figure 6: Temporal waveforms of the optical frequency. The black solid and red dashed curves represent the laser 1 and 2, respectively.

$(n_{s1} + n_{s2})/2$. From Fig. 5, the averaged trajectory itinerates on the lower steady state solutions although the trajectories of the two lasers do not itinerate on the steady state solutions in Fig. 4.

To investigate the frequency dynamics of the two lasers, we observe the temporal waveforms of the optical frequencies $f_1(t)$ and $f_2(t)$ as shown in Figure 6. The black solid and red dashed curves represent the laser 1 and 2, respectively. Both $f_1(t)$ and $f_2(t)$ start decreasing at $t \approx 30$ ns, and the sign of $f_1(t) - f_2(t)$ changes in time for each propagation delay time. In the LFF dynamics of a single laser with optical feedback, the optical frequency of the single laser decreases monotonically along the steady state solutions [9, 13]. However, we found that the optical frequencies of the mutually-coupled lasers move up and down in Fig. 6. This result indicates that the optical frequency of one laser pulls that of the other laser with time delay, and the role of the frequency pulling effect is exchanged in time.

The dynamics of LFFs and the propagation delay time are important for the observation of the short-term exchange of the leader-laggard relationship. The trajectories of the two coupled lasers moves along the averaged steady state solutions. Although the mutually-coupled lasers do not have complete synchronized solutions due to the existence of the optical frequency detuning, the two lasers move along the frequency-locked steady state solutions. However, frequency locking is not always achieved since the optical frequencies of the two lasers change in time due to the propagation delay time. The interplay of the frequency locking between the mutually coupled lasers results in the short-term exchange of the leader-laggard relationship.

5. Conclusions

We investigated the short-term exchange of the leader-laggard relationship in mutually-coupled semiconductor lasers. The two lasers show LFF dynamics and one of the laser always has intensity dropouts in advance, which is the leader, due to the existence of the optical frequency detuning. We observed the short-term exchange of the leader-laggard relationship by using short-term cross-correlations. We also calculated the steady state solutions, which are frequency locked solutions, for the mutually-coupled semiconductor lasers to investigate the mechanism of the short-term exchange of the leader-laggard relationship. We found that the averaged trajectory for the two coupled lasers in the phase space itinerates on the steady state solutions, and the optical frequency locking alternately occurs in the two lasers. The short-term exchange of the leader-laggard relationship could be a general phenomenon for mutually-coupled dynamical systems with time delay.

References

[1] L.M. Pecora and T.L. Carroll, Phys. Rev. Lett., vol. 64, pp. 821–824 (1990).
[2] S. Boccaletti, J. Kurths, G. Osipov, D.L. Valladares, and C.S. Zhou, Physics Reports, vol. 366, no. 1–2, pp. 1–101 (2002).
[3] M.C. Soriano, J. García-Ojalvo, C.R. Mirasso, and I. Fischer, Rev. Mod. Phys., vol. 85, pp. 421–470 (2013).
[4] A. Uchida, Optical Communication with Chaotic Lasers, Applications of Nonlinear Dynamics and Synchronization, Wiley-VCH, Weinheim, 2012.
[5] T. Heil, I. Fischer, W. Elsässer, J. Mulet, and C.R. Mirasso, Phys. Rev. Lett., vol. 86, pp. 795–798 (2001).
[6] K. Hicke, O. D'Huys, V. Flunkert, E. Schöll, J. Danckaert, and I. Fischer, Phys. Rev. E, vol. 83, pp. 056211–1–11 (2011).
[7] M. Ozaki, H. Someya, T. Mihara, A. Uchida, S. Yoshimori, K. Panajotov, and M. Sciamanna, Phys. Rev. E, vol. 79, pp. 026210 (2009).
[8] T. Hida, K. Kanno, and A. Uchida, Proceedings of 2012 the International Symposium on Nonlinear Theory and Its Applications, vol.1, pp. 399–402 (2012).
[9] T. Sano, Phys. Rev. A, vol. 50, pp. 2719–2726 (1994).
[10] I. Fischer, G.H.M. vanTartwijk, A.M. Levine, W. Elsässer, E. Göbel, and D. Lenstra, Phys. Rev. Lett., vol. 76, pp. 220–223 (1996).
[11] R. Lang and K. Kobayashi, IEEE J. Quantum Electron., vol. 16, pp. 347–355 (1980).
[12] K. Kanno and A. Uchida, Phys. Rev. E, vol. 86, pp. 066202–1–9 (2012).
[13] A.P. Bogatov, P.G. Eliseev, and B.N. Sverdlov, IEEE J. Quantum Electron., vol. 11, no. 7, pp. 510–515 (1975).